

# Poly(vinyl alcohol-vinyl acetate) Copolymer Hydrogels: Scattering and Osmotic Observations

Ferenc Horkay,<sup>\*,†,‡</sup> Walther Burchard,<sup>†</sup> Anne-Marie Hecht,<sup>§</sup> and Erik Geissler<sup>§</sup>

*Institut für Makromolekulare Chemie, Universität Freiburg, Stefan Meier Strasse 31, D-7800 Freiburg i. Brsg., FRG, Department of Colloid Science, Eötvös Loránd University, Pázmány Péter sétány 2, Pf. 32, H-1518 Budapest, Hungary, and Laboratoire de Spectrométrie Physique (CNRS associate lab), Université Joseph Fourier de Grenoble, B.P. 87, F-38402 St Martin d'Hères, France*

Received December 14, 1992; Revised Manuscript Received March 22, 1993

**ABSTRACT:** Light and small angle X-ray scattering measurements have been made on chemically cross-linked poly(vinyl alcohol-vinylacetate) copolymer hydrogels and on the corresponding semidilute solutions. The results of these observations are compared with elastic and osmotic measurements performed on the same networks. The variation of the intensity of the dynamic component of the scattered light was investigated as a function of the cross-linking density. At low cross-linking density, the observed intensity arising from concentration fluctuations in the gel exceeds that of the corresponding solution, while at higher cross-linking density the opposite is true. In the solution, the intensity correlation function exhibits two well-separated relaxation processes, both of which are diffusive; i.e. the relaxation rates vary as  $Q^2$ . The fast relaxation process describes the cooperative motions of the polymer in the solvent.

## Introduction

Recently, several investigations have been performed to determine the scattering and osmotic properties of various hydrogels.<sup>1-6</sup>

However, owing to specific interactions in aqueous solutions, e.g. hydrogen bonding or associations of ionic groups, hydrogels generally favor the formation of clusters or other superstructures. Usually such processes are time dependent, with the result that the equilibrium properties are poorly defined. The large size range of molecular superstructures in poly(vinyl alcohol)-water has been observed by small angle neutron scattering.<sup>2</sup>

In a recent paper<sup>6</sup> we investigated the osmotic and light scattering behavior of poly(vinyl alcohol) hydrogels and solutions. A comparison was made between the static light scattering response of this system with that of a poly(vinyl alcohol-vinyl acetate) copolymer in water. It was found that presence of the acetate groups significantly influences the static structure of both gel and solution. These modifications are accompanied by changes in the concentration dependence of the elastic modulus. In contrast to PVA-water, over the time scale of the observations, the copolymer system exhibits no significant variation in its static scattering properties.

In this paper we report measurements of dynamic and static light scattering, small angle X-ray scattering (SAXS), as well as osmotic swelling pressure and elastic modulus in the poly(vinyl alcohol-vinyl acetate) (P(VA-VAc)) hydrogel system, prepared by random chemical cross-linking. The effect of cross-linking density on the intensity and relaxation rates of the dynamically scattered light was investigated.

The osmotic and scattering properties of aqueous P(VA-VAc) copolymer gels are compared with those of P(VA-VAc) copolymer solutions.

## Theoretical Background

**Thermodynamic Description.** In agreement with previous experimental evidence,<sup>7-12</sup> we adopt the assumption of Flory and Rehner<sup>13</sup> that the free energy of a swollen network can be expressed as the sum of a mixing and an elastic component

$$\Delta F_{\text{tot}} = \Delta F_{\text{mix}} + \Delta E_{\text{net}} \quad (1)$$

In distinction to the assumption of ref 13, however,  $\Delta F_{\text{mix}}$  may differ significantly from that of the solution.<sup>7-12</sup> Theoretical attempts, based on modifications to the polymer-solvent interaction in the vicinity of the cross-link points, have been proposed<sup>14,15</sup> to explain such differences.

In an osmotic experiment, the observable quantities involve the derivative of  $\Delta F_{\text{mix}}$ , which, with a Flory-Huggins type equation,<sup>16</sup> can be expressed as

$$\Pi = -\partial\left(\frac{\Delta F_{\text{mix}}}{v}\right)/\partial n_1 = - (RT/v)[\ln(1-\varphi) + (1-P^{-1})\varphi + \chi\varphi^2 + w\varphi^3] \quad (2)$$

Here  $\Pi$  is the osmotic pressure,  $n_1$  is the number of moles of solvent,  $\varphi$  is the polymer volume fraction,  $v$  is the molar volume of the solvent,  $\chi$  and  $w$  are interaction parameters, and  $P$  is the degree of polymerization (for a cross-linked polymer  $P = \infty$ ).

According to scaling considerations,<sup>17</sup> the osmotic pressure of a polymer solution in the semidilute regime exhibits a power law behavior

$$\Pi = A\varphi^n \quad (3)$$

where  $A$  is a constant, and  $n \approx 9/4$  in good solvent conditions.

The theory of rubber elasticity<sup>18,19</sup> yields for the elastic modulus  $G$

$$G = \partial\left(\frac{\Delta F_{\text{net}}}{v}\right)/\partial n_1 = kT\zeta\varphi^{1/3} \quad (4)$$

where  $\zeta$  is the cycle rank of the network.

**Scattering Considerations.** At small values of the transfer wave vectors  $Q [= (4\pi n/\lambda) \sin(\theta/2)]$ , where  $n$  is the refractive index of the medium,  $\lambda$  is the wavelength of the

\* Author to whom correspondence should be addressed at Universität Freiburg.

† Universität Freiburg.

‡ Eötvös University.

§ Université Joseph Fourier de Grenoble.

incident radiation, and  $\theta$  is the scattering angle], the elastic scattering intensity from a neutral polymer solution is<sup>17</sup>

$$I(Q) = a \frac{kT(\rho_p - \rho_s)^2 \varphi^2}{K_{os}} \frac{1}{1 + Q^2 \xi^2} \quad (5)$$

where  $a$  is an apparatus constant,  $\xi$  is the concentration correlation length, and  $(\rho_p - \rho_s)^2$  is a contrast factor. In an X-ray scattering experiment  $\rho_p$  and  $\rho_s$  are the electron densities of the polymer and the solvent, respectively. In a light scattering experiment the contrast factor is given by  $16\pi^2 n_0^2 (\partial n / \partial \varphi)^2 / (\alpha \rho^2 \lambda^4)$ , where  $n_0$  is the refractive index of the solvent and  $\rho$  is the polymer mass density. The quantity  $K_{os} = \varphi (\partial \Pi / \partial \varphi)$  is the osmotic compressional modulus of the solution.

For gels, owing to their finite elasticity, the osmotic pressure  $\Pi$  is replaced by the swelling pressure,  $\omega$ . The scattered intensity is then governed by the longitudinal osmotic modulus<sup>20</sup>

$$M_{os} = \varphi \partial \omega / \partial \varphi + (4/3)G \quad (6)$$

where  $G$  is the shear modulus of the swollen network.

In light scattering experiments the intensity arising from concentration fluctuations in a polymer solution is expressed in terms of the Rayleigh ratio  $R(\theta)$

$$R(\theta) = R(\theta)_{\text{solution}} - R(\theta)_{\text{solvent}} = RTK\varphi / (\partial \Pi / \partial \varphi) \quad (7)$$

where  $K = 16\pi^2 n_0^2 (\partial n / \partial \varphi)^2 / (\rho^2 \lambda^4 N_A)$  and  $N_A$  is Avogadro's number.

In gels the scattered intensity at small  $Q$  is usually greater than in the corresponding polymer solutions. Excess intensity is scattered by permanent concentration fluctuations in the network structure resulting from local variations in cross-linking density. This concentration polydispersity is an analog of molecular weight polydispersity encountered in dilute polymer solutions. The thermodynamics of polymer gels are, however, principally governed by the short range concentration fluctuations in the system.<sup>5,21-23</sup>

## Experimental Section

**Sample Preparation.** Gels were prepared in aqueous solutions by cross-linking P(VA-VAc) linear copolymer with glutaraldehyde<sup>24</sup> at pH = 1.5. For the experiments a fractionated polymer sample was used ( $M_w^{\text{P(VA-VAc)}} = 128\,000$ ), where the acetate content was 12% (mol/mol). The copolymer was prepared by equilibrium reacylation of a fully hydrolyzed poly(vinyl alcohol) sample which yields the most random distribution of acetate groups.<sup>25</sup> Cross-links were introduced at polymer weight fractions 3.0, 4.0, 5.0, 6.0, 7.0, and 8.0% (w/w). The molar ratio of monomer units to the molecules of cross-linker was 200 at each concentration. For the 6% gel, a series of samples with different molar ratios (200, 150, and 100) were synthesized.

For the calculation of the polymer volume fractions,  $\varphi$ , the densities of the pure components ( $\rho_{\text{P(VA-VAc)}} = 1.246 \text{ g cm}^{-3}$  and  $\rho_{\text{water}} = 0.9971 \text{ g cm}^{-3}$ ) were used.

**Swelling and Mechanical Measurements.** The swelling pressure of the gels was obtained as a function of  $\varphi$  using a modified deswelling method,<sup>26</sup> whereby gels were equilibrated with aqueous poly(vinyl pyrrolidone) ( $M_n = 29\,000$ ) solutions of known osmotic pressure.<sup>27</sup> A semipermeable membrane between the gel and the solution prevented diffusion of the polymer molecules into the swollen network.

The shear modulus measurements were performed on isometric cylindrical gel specimens prepared in a special mould. Swollen networks were uniaxially compressed (at constant volume) between two parallel flat plates.<sup>28</sup> The stress-strain data were determined in the range of deformation ratio  $0.7 < \Lambda < 1$ . No volume change or barrel distortion was detected.

**Light Scattering.** Static and dynamic light scattering experiments were performed using an ALV/SP-86 automatic

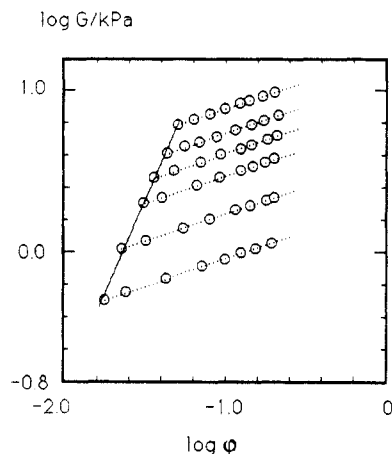


**Figure 1.** Double logarithmic plot of the shear modulus  $G$  as a function of deswelling in six P(VA-VAc) gels prepared at different concentrations. The dotted straight lines through the data sets from each gel give the power law behavior of the modulus in the concentration range  $\varphi \leq 0.18$ . The slope of these lines is  $0.33 \pm 0.01$ . The steep continuous line shown through the data at equilibrium swelling with the pure diluent has a slope of 2.3.

goniometer (ALV, Langen, Germany) at 25 °C in the range of angles  $30^\circ \leq \theta \leq 150^\circ$ . A Spectra Physics 2020 krypton ion laser working at  $\lambda = 647.1 \text{ nm}$  was used at a power level of approximately 300 mW. The intensity correlation functions were accumulated on an ALV-3000 multibit correlator. The analysis of the correlation function was performed by inverse Laplace transformation using the CONTIN<sup>29</sup> routine.

The solution and the gel samples were prepared in Hellma cylindrical cells of inner diameter 8 mm. Dust was removed by filtering the homogenized solutions directly into the light scattering cells through Millipore filters of pore size  $0.45 \mu\text{m}$ . The sample cell in the goniometer was surrounded by a refractive index-matching bath (decalin), which was thermostated by circulating water. For the absolute intensity calibration the scattering from pure toluene was measured.

During the static light scattering measurements the sample cells were rotated continuously in the goniometer unit to ensure full averaging of the scattered light intensity. In the dynamic measurements the intensity correlation function and the static scattered intensity were determined simultaneously at fixed positions of the sample.

For the experimental setup the collection optics coherence factor,  $\beta$ , was found to be  $0.93 \pm 0.02$ .

**Synchrotron Radiation Scattering.** The X-ray scattering measurements were made on the D24 instrument on the DCI synchrotron at LURE Orsay. The incident wavelength was  $1.608 \text{ \AA}$ .

The solution and the gel samples were contained in cells consisting of thin mica windows sealed in an air-tight stainless steel housing to prevent evaporation of the solvent. The spacing between the windows was defined by a 1 mm thick stainless steel washer. An 18 cm linear gas filled detector with a resolution of 512 points was situated at 170 cm from the sample, and an evacuated tube with Kapton windows was placed in the intervening space. To minimize the possibility of radiation damage to the samples, short exposure times (ca. 900 s) were used.

The sample blanks for background subtraction consisted of pure water contained in the same cell as was used for the sample measurement; this procedure ensured that sample and background had identical thickness.<sup>5,22</sup>

All the experiments were conducted at 25 °C.

## Results and Discussion

**Swelling and Mechanical Results.** In Figure 1 the shear moduli of the P(VA-VAc) gels are displayed as a function of polymer volume fraction in a double logarithmic plot. In this representation, according to eq 4, the slopes of the straight lines through data sets from each sample (dotted lines in Figure) should display a slope of 1/3. The

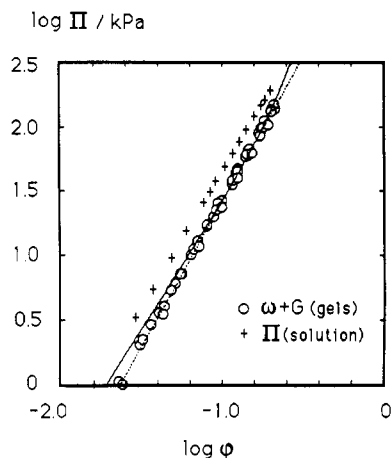


**Figure 2.** Double logarithmic plot of the osmotic pressure of the P(VA-VAc) solutions (crosses) and the sum ( $\omega + G$ ) for the gels (circles) as a function of polymer volume fraction  $\phi$ . The continuous line is the fit of eq 2 to the gel data points and the dotted line is that of eq 3.

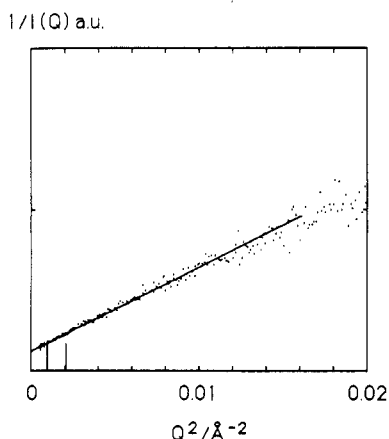


**Figure 3.** Zimm representation of the SAXS spectrum for a P(VA-VAc) solution at  $\phi = 0.1026$ . The continuous straight line is the fit to eq 5 of the data points from the region inside the vertical bars shown.

experimental results are in agreement with this value. The continuous curve connecting the lowest concentration points of each data set has a slope 2.3, in close agreement with the scaling exponent  $9/4$  expected for fully swollen gels.<sup>17</sup>

With the additivity assumption for the elastic and mixing free energy terms as in eq 1, the osmotic component of the swelling pressure,  $\Pi_{\text{mix}}$ , in the swollen network can be expressed as

$$\Pi_{\text{mix}} = \omega + G \quad (8)$$

where the measured values of  $G$  are shown in Figure 1. In Figure 2,<sup>4</sup> both the osmotic pressure  $\Pi$  of the un-cross-linked P(VA-VAc)/water solutions and ( $\omega + G$ ) for the gels are plotted as a function of  $\phi$ . The data from the solutions lie higher than those of the gels. In this figure, the results from all the gel samples prepared at different polymer concentrations are represented by the same symbol (open circles). Within the experimental error, all these points fall on a single master curve. The least-squares fits of ( $\omega + G$ ) to eqs 2 and 3 are shown (continuous line, eq 2, with  $\chi = 0.479$ ,  $w = 0.379$ ; dotted line, eq 3, with  $A = 4602$  kPa,  $n = 2.22$ ). Note that for the gels, the experimental data are represented quite well by both the Flory-Huggins and the scaling expressions.

**SAXS and Static Light Scattering Results.** In Figure 3, the SAXS scattering spectrum from a P(VA-

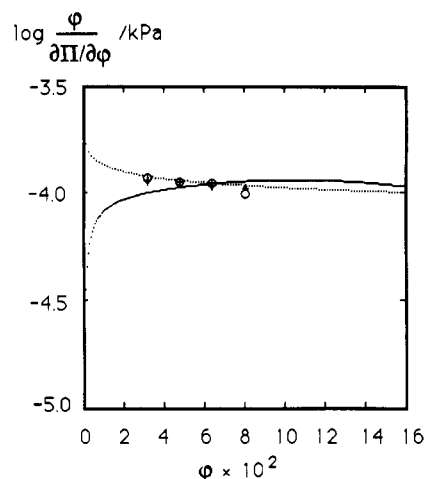


**Figure 4.** Plot of  $\phi/(\partial\Pi/\partial\phi)$  for four P(VA-VAc) solutions as a function of polymer volume fraction: crosses, dynamic light scattering data; circles, SAXS data. The continuous curve is calculated from eq 2, using the parameters determined from the fit shown in Figure 2. The dotted line is calculated from the fit to eq 3.

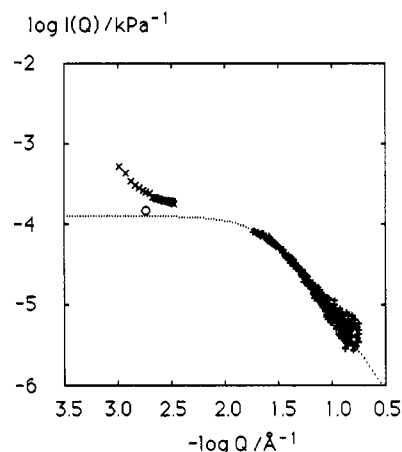


**Figure 5.** Double logarithmic representation of the normalized scattering intensity  $I(Q)$  vs  $Q$  for a P(VA-VAc) gel at  $\phi = 0.0321$ :  $\times$ , static light scattering; +, SAXS;  $\circ$ , dynamic light scattering. The dotted line is the least-squares fit of eq 5 through the SAXS data points.

VAc) solution ( $\phi = 0.1026$ ) is displayed in a Zimm representation. The correlation length determined from this spectrum is  $20.4 \text{ \AA}$ . The straight line through the experimental points is the least-squares fit to eq 5 in the Guinier region ( $Q\xi \leq 1$ ). The vertical bars indicate the limits of the data points used in the fitting procedure. According to eq 5, the intensity at  $Q = 0$  is inversely proportional to the osmotic compressional modulus of the solution. At the concentration of this sample the value of this modulus, calculated from the solution data of Figure 2, is  $K_{\text{os}} = 64.5$  kPa.

In Figure 4 the normalised SAXS (circles) and dynamic light scattering (crosses) intensities are displayed for P(VA-VAc) solutions at four concentrations. The continuous line shows the variation of  $\phi/(\partial\Pi/\partial\phi)$  calculated from eq 2 with the parameters  $\chi = 0.463$  and  $w = 0.411$  obtained from the osmotic pressure data. The dotted line is the corresponding function calculated from eq 3, with parameters  $A = 5791$  kPa and  $n = 2.11$  from the fit to the same osmotic data.

A typical light scattering spectrum of a gel ( $\phi = 0.0321$ ) is shown in Figure 5 (denoted by the symbol  $\times$ ) together with the SAXS spectrum of the same sample (+). In this figure, the absolute intensity scale of the SAXS spectrum was obtained by normalization with the osmotic com-

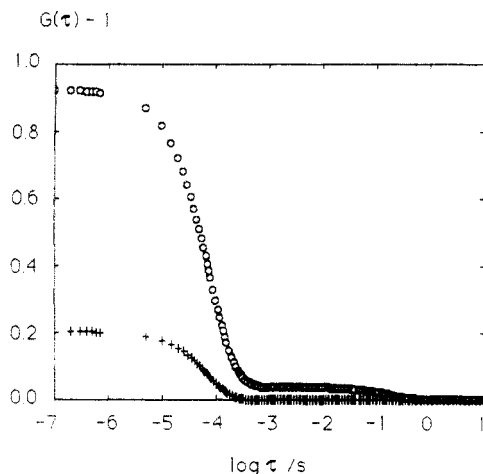


**Figure 6.** Normalized dynamic light scattering intensity correlation functions  $G(\tau) - 1$  from P(VA-VAc) solution (O) and gel (+) at  $\phi = 0.0402$ . Scattering angle,  $\theta = 90^\circ$ .

pressibility<sup>6</sup> of the P(VA-VAc) solution for which the SAXS spectrum is shown in Figure 3. The dotted line is the least-squares fit of the SAXS data points in the Guinier region to eq 5. It can also be seen from the figure that the static light scattering data points lie significantly above the value of  $I(Q)$  extrapolated from the SAXS spectrum. The pronounced angular dependence of the scattered light intensity betrays the presence of structural nonuniformities, the characteristic size of which is comparable with the incident wavelength. As the light scattering spectra are increasingly dominated at smaller  $Q$  vectors by large static superstructures that scatter light more strongly than the dynamic concentration fluctuations,<sup>30,31</sup> the static scattering intensity cannot be related to the thermodynamic properties in a straightforward way. The fitting procedure to the SAXS data assumes that the large scale static nonuniformities do not make their influence felt in the high  $Q$  region, i.e. in the region where the scattering spectrum is dominated by the polymer-polymer correlation length.

**Quasielastic Light Scattering.** In Figure 6 the intensity correlation functions  $G(\tau) - 1$  at scattering angle  $\theta = 90^\circ$  are shown for a P(VA-VAc) solution and the corresponding gel ( $\phi = 0.0402$ ). In this figure, it can be seen that the initial amplitude of the correlation function  $G(0) - 1$  for the gel spectrum is severely reduced and that only one relaxation mode is present.

Analysis of the intensity correlation function  $G(Q, \tau)$  for a solution of diffusing particles can be performed according to the homodyne scheme whereby<sup>32</sup>

$$G(Q, \tau) = 1 + \beta [g(Q, \tau)]^2 \quad (9)$$

where  $g(Q, \tau)$  is the normalized field correlation function and  $\beta$  is the coherence factor ( $\beta \leq 1$ ).

In a system containing static nonuniformities, the detection mode becomes heterodyned, with a resulting intensity correlation function given by<sup>33,34</sup>

$$G(Q, \tau) = 1 + \beta [2X(1 - X)g(Q, \tau) + X^2g(Q, \tau)^2] \quad (10)$$

where  $\tau$  is the delay time and  $X = I_{\text{dyn}}(Q)/I_{\text{tot}}(Q)$ . Here,  $I_{\text{dyn}}(Q)$  is the time average of the intensity of the dynamic component and  $I_{\text{tot}}(Q)$  is that of the total scattered intensity. As mentioned above and illustrated in Figure 5, the static light scattering intensity from the P(VA-VAc) hydrogels is much stronger than that due to concentration fluctuations. A visible consequence of this heterodyning is the reduction of the initial amplitude of intensity correlation function  $G(Q, 0)$ , as is apparent for

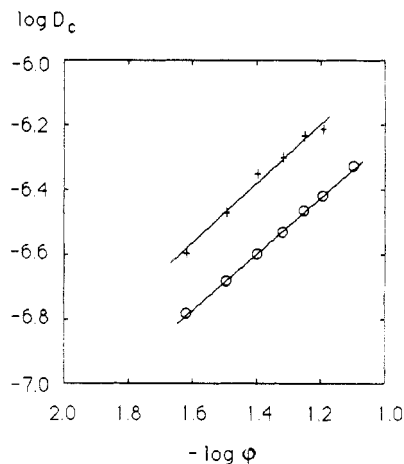


**Figure 7.** Double logarithmic plot of the collective diffusion coefficient  $D_c$  as a function of polymer volume fraction  $\phi$  for P(VA-VAc) solutions (O) and gels (+). The lines shown are the least-squares fits through the respective experimental points.

the gel spectrum displayed in Figure 6. For this particular spectrum the ratio  $X = 0.12$ . Thus the analysis of the gel correlation functions requires the use of eq 10. It was found that the gel spectra could be satisfactorily represented by a single relaxation time. The analysis, based either on CONTIN coupled with a correction for heterodyning according to eq 10 or on a single exponential fitting procedure, yielded identical values of the relaxation rates to within 5%.

In Figure 6, for the solution, two relaxation processes can be seen, differing by more than 3 orders of magnitude. Both of these relaxation rates,  $\Gamma_{\text{fast}}$  and  $\Gamma_{\text{slow}}$ , are proportional to  $Q^2$ , i.e. both are diffusive processes.

The collective diffusion coefficient  $D_c$  is related to  $\Gamma_{\text{fast}}$  through<sup>35</sup>

$$D_c = \Gamma_{\text{fast}}/Q^2(1 - \phi)^2 \quad (11)$$

where the factor  $(1 - \phi)^{-2}$  takes account of center of mass motion and the symmetry of the kinetic coefficients.<sup>36</sup> The resulting values of  $D_c$  for the gels and solutions are displayed as a function of polymer volume fraction in a double logarithmic representation in Figure 7. Within the experimental accuracy, both solutions and gels exhibit similar behavior. The slopes of the least-squares straight line fits through the data points are 0.87 and 0.91, respectively. These values are in excess of the scaling prediction (slope = 0.77) for polymer solutions in good solvent conditions.<sup>17</sup> The ratio  $D_c^{\text{gel}}/D_c^{\text{sol}}$  is approximately 1.5 for the present system. A similar ratio between the collective diffusion coefficients has been reported recently for PDMS gels and solutions.<sup>37</sup> Since the diffusion coefficient for the gel can be expressed in the form<sup>20</sup>

$$D_c^{\text{gel}} = M_{\text{os}}/f$$

the results of ref 37 were interpreted in terms of the ratio of the osmotic moduli in the gel and in the solution,  $M_{\text{os}}/K_{\text{os}}^{\text{sol}}$ . This interpretation, applicable only to fully swollen gels, was based on the assumption that the difference between  $M_{\text{os}}$  and  $K_{\text{os}}^{\text{sol}}$  arises solely from the presence of the finite elasticity. As we shall see below, and has been reported for other systems,<sup>5,21-23</sup> the osmotic compressibility of the solution is, however, generally larger than in the corresponding gel. In other words, the assumption that  $K_{\text{os}}^{\text{gel}} = K_{\text{os}}^{\text{sol}}$  is an oversimplification.<sup>38</sup>

The slow relaxation process,  $\Gamma_{\text{slow}}$ , which decreases with increasing polymer volume fraction (Figure 8), has been identified with the translational motion of clusters of

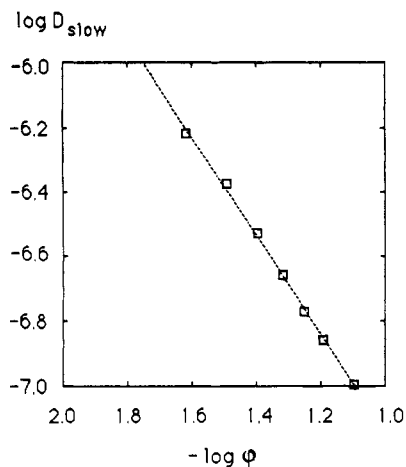


**Figure 8.** Double logarithmic plot of the slow diffusion coefficient  $D_{\text{slow}}$  as a function of polymer volume fraction  $\phi$  for the P(VA-VAc) solutions. The straight line is the least-squares fit through the experimental points.

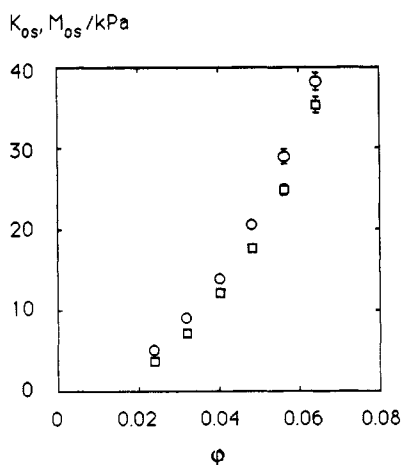


**Figure 9.** Plot of the osmotic compressional moduli  $K_{\text{os}}$  of the solutions (circles) and of the longitudinal osmotic moduli  $M_{\text{os}}$  of the gels (squares) as a function of polymer volume fraction  $\phi$  for the P(VA-VAc) system.

macromolecules through the entangled polymer matrix.<sup>3,39</sup> In the observed concentration range  $D_{\text{slow}}$  coincides with a power law dependence, with an apparent exponent  $-3$ . For the gel, absence of a slow relaxation process results from the fact that network chains no longer undergo translational diffusion.

**Integrated Intensity Measurements.** Analysis of the correlation function using eq 10 allows the determination of the ratio  $X$  and, thereby, yields the intensity of the scattered light associated with the dynamic concentration fluctuations,  $I_{\text{dyn}}(Q)$ . The error in the resulting estimate for the osmotic modulus is not better than 5%.

The value of  $I_{\text{dyn}}(Q)$  obtained from the correlation function at  $\theta = 90^\circ$  of the gel sample with  $\phi = 0.0321$  is shown as an open circle in Figure 5. This point lies close to the plateau of the theoretical (Lorentzian) curve calculated from X-ray scattering. In view of the experimental uncertainties involved in the different measurements, the agreement between the dynamic light scattering result and that of SAXS is acceptable.

From the intensity  $I_{\text{dyn}}(Q)$  scattered by concentration fluctuations, eq 5 allows the osmotic modulus,  $K_{\text{os}}$  or  $M_{\text{os}}$ , of the system to be calculated. In Figure 9 the values of  $K_{\text{os}}$  of the solutions and  $M_{\text{os}}$  of the gels, obtained from dynamic light scattering, are plotted as a function of polymer volume fraction. It can be seen that  $K_{\text{os}}^{\text{sol}} > M_{\text{os}}$  over the whole concentration range studied.

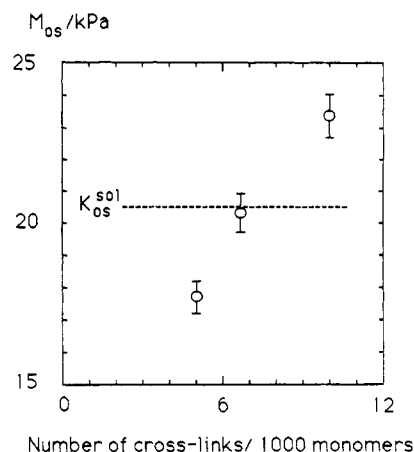


**Figure 10.** Variation of the longitudinal modulus  $M_{\text{os}}$  of a P(VA-VAc) gel ( $\phi = 0.0482$ ) with cross-linking density. The dotted horizontal line designates the value of the osmotic compressional modulus  $K_{\text{os}}^{\text{sol}}$  for the solution at the same concentration.

In the gel,  $M_{\text{os}}$  contains two contributions,<sup>38</sup>  $K_{\text{os}}^{\text{gel}}$  and  $G$ . The latter is absent from the solution and, therefore, cannot be the cause of the shortfall in  $M_{\text{os}}$  with respect to  $K_{\text{os}}^{\text{sol}}$ . The observed reduction of  $M_{\text{os}}$  upon cross-linking can therefore only be attributed to a decrease in the osmotic component. Gel systems in general exhibit local variations in cross-linking density which on swelling generate polydispersity in the concentration. Consequently the movement of polymer segments belonging to more densely cross-linked regions cannot participate fully in the concentration fluctuations that control the thermodynamic properties. Therefore the apparent value of  $K_{\text{os}}^{\text{gel}}$  becomes smaller than  $K_{\text{os}}^{\text{sol}}$ . It is expected that  $K_{\text{os}}^{\text{gel}}$  will depend not only on the polymer-solvent interaction but also on the density and the distribution of the cross-links in the network.

In Figure 10 are shown the values of  $M_{\text{os}}$  for the gels at  $\phi = 0.0482$  at three different degrees of cross-linking. The horizontal straight line denotes the osmotic compressional modulus of the corresponding solution ( $K_{\text{os}}^{\text{sol}} = 20.6$  kPa).  $M_{\text{os}}$  increases with cross-linking density and, at the highest cross-linking density investigated, exceeds  $K_{\text{os}}^{\text{sol}}$ .

## Conclusions

In the P(VA-VAc) gels investigated, the osmotic pressure of the polymer in the network is slightly smaller than that of the corresponding polymer solution at identical concentration.

In the gels the presence of large scale nonuniformities heterodynes the light scattered by the concentration fluctuations. In the solutions, two relaxation processes can be discerned, both of which are diffusive. The cooperative diffusion coefficient of the gels follows a similar concentration dependence to that of the solutions but their numerical values are about 50% larger.

At the lowest cross-linking density explored, the longitudinal osmotic modulus  $M_{\text{os}}$  of the gels is systematically smaller than the osmotic compressional modulus  $K_{\text{os}}^{\text{sol}}$  of the solution at the same concentration. The difference ( $K_{\text{os}}^{\text{sol}} - M_{\text{os}}$ ) depends on the cross-linking density and changes sign for high cross-linking densities.

**Acknowledgment.** F.H. acknowledges a research fellowship from the Alexander von Humboldt Stiftung. We are grateful to the Laboratoire de l'Utilisation du Rayonnement Electromagnétique (LURE), Orsay, for beam time on the D24 instrument. This work is part of a joint CNRS-Hungarian Academy of Sciences project.

We also acknowledge research Contract OTKA No. 2158 from the Hungarian Academy of Sciences.

### References and Notes

- (1) Mallam, S.; Horkay, F.; Hecht, A.-M.; Geissler, E. *Macromolecules* **1989**, *22*, 3356.
- (2) Wu, W.; Shibayama, M.; Roy, S.; Kurokawa, H.; Coyne, L. D.; Nomura, S.; Stein, R. S. *Macromolecules* **1990**, *23*, 2245.
- (3) Fang, L.; Brown, W. *Macromolecules* **1990**, *23*, 3284.
- (4) Joosten, J. G. H.; McCarthy, J. L.; Pusey, P. N. *Macromolecules* **1991**, *24*, 6690.
- (5) Geissler, E.; Horkay, F.; Hecht, A. M. *Macromolecules* **1991**, *24*, 6006.
- (6) Horkay, F.; Burchard, W.; Geissler, E.; Hecht, A.-M. *Macromolecules* **1993**, *26*, 1296.
- (7) Horkay, F.; Zrinyi, M. *Macromolecules* **1982**, *15*, 1306.
- (8) McKenna, G. B.; Flynn, K. M.; Chen, Y. *Polym. Commun.* **1988**, *29*, 272.
- (9) Horkay, F.; Hecht, A.-M.; Geissler, E. *J. Chem. Phys.* **1989**, *91*, 2706.
- (10) Geissler, E.; Horkay, F.; Hecht, A.-M.; Zrinyi, M. *J. Chem. Phys.* **1989**, *90*, 1924.
- (11) McKenna, G. B.; Flynn, K. M.; Chen, Y. *Macromolecules* **1989**, *22*, 4507.
- (12) McKenna, G. B.; Flynn, K. M.; Chen, Y. *Polymer* **1990**, *31*, 1937.
- (13) Flory, P. J.; Rehner, J., Jr. *J. Chem. Phys.* **1943**, *11*, 521.
- (14) Neuburger, N. A.; Eichinger, B. E. *Macromolecules* **1988**, *21*, 3060.
- (15) Freed, K. F.; Pesci, A. I. *Macromolecules* **1989**, *22*, 4048.
- (16) Flory, P. J. *Principles of Polymer Chemistry*; Cornell University Press: Ithaca, NY, 1953.
- (17) de Gennes, P. G. *Scaling Concepts in Polymer Physics*; Cornell University Press: Ithaca, NY, 1979.
- (18) James, H. M.; Guth, E. J. *J. Chem. Phys.* **1943**, *11*, 455.
- (19) Treloar, L. R. G. *The Physics of Rubber Elasticity*, 3rd ed.; Clarendon: Oxford, 1975.
- (20) Tanaka, T.; Hocker, L. O.; Benedek, G. B. *J. Chem. Phys.* **1973**, *59*, 5151.
- (21) Horkay, F.; Hecht, A.-M.; Mallam, S.; Geissler, E.; Rennie, A. R. *Macromolecules* **1991**, *24*, 2896.
- (22) Hecht, A.-M.; Horkay, F.; Geissler, E.; Benoit, J. P. *Macromolecules* **1991**, *24*, 4183.
- (23) Hecht, A.-M.; Guillermo, A.; Horkay, F.; Mallam, S.; Legrand, J. F.; Geissler, E. *Macromolecules* **1992**, *25*, 3677.
- (24) Horkay, F.; Nagy, M. *Polym. Bull.* **1980**, *3*, 457.
- (25) Toyashima, K. In *Polyvinyl Alcohol, Properties and Applications*; Finch, C. A., Ed.; John Wiley and Sons: London, 1973.
- (26) Nagy, M.; Horkay, F. *Acta Chim. Acad. Sci. Hung.* **1980**, *104*, 49.
- (27) Vink, H. *Eur. Polym. J.* **1971**, *7*, 1411.
- (28) Horkay, F.; Nagy, M.; Zrinyi, M. *Acta Chim. Acad. Sci. Hung.* **1980**, *103*, 387.
- (29) Provencher, S. W. CONTIN (Version 2), Göttingen, 1984.
- (30) Geissler, E.; Hecht, A.-M.; Duplessix, R. *J. Polym. Sci., Polym. Phys. Ed.* **1982**, *20*, 225.
- (31) Soni, V. K.; Stein, R. S. *Macromolecules* **1990**, *23*, 5257.
- (32) Berne, B. J.; Pecora, R. *Dynamic Light Scattering*; Wiley-Interscience: New York, 1976.
- (33) Pusey, P. N.; van Megen, W. *Physica A* **1989**, *157*, 705.
- (34) Geissler, E. In *Dynamic Light Scattering, the Method and Some Applications*; Brown, W., Ed.; Oxford University Press: Oxford, 1993.
- (35) Vink, H. *J. Chem. Soc., Faraday Trans.* **1985**, *81*, 1725.
- (36) Landau, L. D.; Lifshitz, E. M. *Fluid Mechanics*; Pergamon: Oxford, 1976.
- (37) Patel, S. K.; Cohen, C. *Macromolecules* **1992**, *25*, 5252.
- (38) The definition used here for the osmotic modulus,  $K_{os}^{gel} = \varphi \partial \Pi_{mix} / \partial \varphi$ , eliminates the elastic contribution. Hence,  $K_{os}^{gel}$  and  $K_{os}^{sol}$ , being both of purely osmotic origin, are comparable quantities. In this convention, the longitudinal modulus (eq 6) becomes  $M_{os} = K_{os}^{gel} + G$ .
- (39) Matthiez, P.; Mouttet, G.; Weissbuch, G. *J. Phys. (Paris)* **1980**, *41*, 519.